ISSN 1068-3755, Surface Engineering and Applied Electrochemistry, 2017, Vol. 53, No. 3, pp. 285–294. © Allerton Press, Inc., 2017.
Original Russian Text © V.B. Tarel'nik, A.V. Paustovskii, Yu.G. Tkachenko, V.S. Martsinkovskii, E.V. Konoplyanchenko, K. Antoshevskii, 2017, published in Elektronnaya Obrabotka Materialov, 2017, No. 3, pp. 72–81.

# Electric-Spark Coatings on a Steel Base and Contact Surface for Optimizing the Working Characteristics of Babbitt Friction Bearings

**V. B. Tarel'nik[a], *, A. V. Paustovskii[b], Yu. G. Tkachenko[b], **, V. S. Martsinkovskii[a], E. V. Konoplyanchenko[a], and K. Antoshevskii[c], *****

[a] *Sumy National Agricultural University, Sumy, 40021 Ukraine*

[b] *Frantsevich Institute of Problems of Materials Science, National Academy of Sciences of Ukraine, Kyiv, 03680 Ukraine*

[c] *Politechnika Świętokrzyska, Kielce, 25-314 Poland*

**e-mail: tarelnik@i.ua*

***e-mail: tkachenko_yuri@ukr.net*

****e-mail: ktrka@tu.kielce.pl*

Received July 4, 2016

**Abstract**—It is found that the use of transition layers of copper, coated by the electric-spark method in a protective argon atmosphere, improves the heat removal from the contact area and increases the steel bases' adhesion strength with an antifriction babbitt layer as compared with the traditional technology by 35%. Electric-spark alloying babbitt B83 by indium and stannum allowed us to form running-in coatings without hard inclusions with a thickness of 130 and 100 microns, respectively. New technological solutions allow decreasing the temperature in the friction zone, increasing the thickness of the oil layer, and, as a result, creating a bearing with a better load carrying capability and reliability.

*Keywords*: electric-spark coating, spark discharge energy, mass transfer, babbit friction bearing, strength of adhesion, bearing wear-resistance

**DOI:** 10.3103/S1068375517030140

## INTRODUCTION

According to the statistics, up to 32% of the failures of compressor-turbine units, which are employed in the gas industry, occur due to the operational breakdown of the babbit friction bearings; this is most often caused by the destruction and wear of the antifriction layer of half bearings, which leads to the dynamic instability of the operation of the equipment. The breakdown of friction bearings under normal operational conditions is the consequence of various types of wear, namely, cavitation, abrasive wear, wear due to plastic deformation, and fatigue wear. For this reason, the problem of improving the operational characteristics and increasing the operational life of babbit friction bearings is important and topical.

Babbit is used as the material of the antifriction layer of friction bearings, which are used as steel shaft bearings of systems operating at high loads, due to its strong antifriction properties and ability of running-in with a steel shaft. The structure of babbit represents a soft matrix with the inclusions of the reinforcing phase. The matrix is represented by the $\alpha$-phase (solid solution of Sb and Cu in Sn) and solid inclusions ($\beta$-phase (SnSb), and $\gamma$-phase ($Cu_3Sn$)), which provide high wear resistance [1, 2]. Experience has shown that the quality of the antifriction layer of a bearing must be evaluated by the following criteria: adhesive strength of the coating with the basis, cohesive strength of the antifriction layer, porosity, the degree of residual stresses, and structural homogeneity.

Casting is a conventional method for preparing babbit coatings for friction bearings. However, casting techniques have several drawbacks, which cannot be avoided: low adhesive strength of the coating with the base; formation of clowholes, cast blowholes, and coarsening of grains in the babbit layer; and structural heterogeneity, which is related to the liquation of reinforcing elements along the section of the mold. Everything mentioned above, which represents the stress concentrator, results in the generation of fatigue cracks and the destruction of babbit during the operation of the bearing. Pores and cast blowholes significantly reduce the adhesive strength of babbit with the base material.

With the aim to increase the wear resistance of babbit bearings, studies are being carried out in three main directions. Firstly, improving the casting methods of babbit coatings, which can minimize the number of defects, which are formed in the babbit layer during casting, and in particular, solve the problem of liquation of the reinforcing phase. Other problems are also important, more specifically, the increased adhesive strength of a babbit cast layer with the base and improved heat withdrawal from the friction area, as well as the optimization of the running-in of the steel shaft to the babbit coating.

Under long-term variable loading, fatigue cracks, which arise on the friction surface of a bearing, penetrate inside the layer. A crack opening occurs under the surge in pressure of the lubricating material. After reaching the base of the antifriction layer, the crack changes its direction and propagates along the joint of the base with the layer, which leads to the roughening of the individual section of the surface layer and the formation of surface "pits," which are blocked by the debris from wear-and-tear acting as an abrasive [3]. The resistance to the wear-and-tear of the antifriction layer of babbit bearings depends on the state and properties of the intermediate layer in area where the babbit joins the steel base. Based on the analysis of the existing technologies for fabricating half bearings, investigation of their operating conditions, and reasons for the destruction of the antifriction babbit layer, it was considered reasonable to apply the intermediate layer from copper or tin bronze onto the steel substrate prior to plating by electric-spark alloying (ESA) in order to ensure the strong adhesion of the steel substrate with babbit, as well as to intensify heat withdrawal from the friction zone. The importance of heat withdrawal is related to the fact that a significant drawback of babbits is that all the parameters of their mechanical strength, and in particular, fatigue resistance, decrease with an increase in temperature. The preliminary investigations confirmed that electroerosion, which results in the minimum weld penetration and consistency of the deposited coating [4], is more effective for this purpose than welding deposition, electroplating, metalizing, and ionic bombardment. The formation of a transition layer from copper, which is tightly bonded on one side with the steel substrate and on the other side with the tin layer by the formation of substitutional solid solutions and babbit by the ESA method ensures stronger adhesion of the steel substrate with babbit, as well as a more intense heat withdrawal from the friction area.

The concept of antifrictionality includes the set of parameters that have to be fulfilled by the bearing material. These properties primarily include the ability of easily running-in to the joining detail. During the fabrication of housings and friction half bearings and the assembly of mechanisms, there are always deviations from the ideal geometrical shape. The accumulation of errors reduces the real adhesive area of the shaft to the friction surface of the bearing and thus decreases the damping efficiency and load carrying ability of the friction bearing. During the running-in of the rubbing couple, the true contact area increases due to the elastic and plastic deformation of the surface layer; the friction force, temperature, and the intensity of the wear-and-tear in the contact area increase; and micro- and macrodamage is usually formed on the friction surface. This damage includes the local destruction of the structural components as a result of overloads. As an example, when using B83 babbit in SnSb grains in thin-layer bearings, microcracks are formed, which become the sites of crack propagation in the bulk layer [5]. The formation of indium or a tin coating on the surface of the babbit layer, whose microhardness is less than that of the base, and the absence of solid inclusions improve the running-in conditions of the half bearings to the steel shaft and increase the reliability and life cycle of the friction bearings.

Thus, the aim of this work is to improve the quality of babbit friction bearings by the formation of transition layers by the electric-spark method, which improves heat withdrawal and the adhesive strength of the antifriction babbit layer to the base, as well as the running-in coatings, which increase their operating efficiency and ability to carry heavy loads for a longer time.

## OBJECTS AND METHODS OF STUDY

The specimens with electric-spark coatings obtained on an EILV-8A (Ukraine) equipped with a manual vibrator represent the objects of study. To study the structure and properties of laminar surface layers, electric-spark coatings were deposited both in the air and argon atmosphere onto 10 × 10 × 10 mm specimens from steel 20 in the as-received state (175–180 HV). In this case, various setup conditions were used in the capacity of a storage capacitor of 150 and 300 μF and discharge energy in the range of 0.04–0.68 J. The data on the conditions used in the work are given in Table 1.

Argon was injected into the alloying area by special equipment. The sequence of electroerosion alloying, plating of the specimen surfaces, and electrode materials are given in Table 2.

The erosion of anode and the gain of the cathode were determined gravimetrically on an analytical balance. Weighing operations were performed at 30-s intervals (up to 2 min) and, then at 60-s intervals (up to 4 min). Prior to each weighing, alloying was performed on a new specimen surface. The coating layer thickness was measured by a micrometer, while the surface roughness was measured on a 201 Kalibr model profilograph-profilometer by recording and processing profilograms.

In order to optimize the running-in of the shaft–bearing pair to steel specimens with the babbit layer, indium or tin coatings were deposited by ESA. ESA was conducted in a protective argon atmosphere under mild alloying conditions with the pulse energy of 0.01–0.03 J. The lower boundary of the pulse is

**Table 1.** Operating conditions of modified EILV-8A setup

| Mode no. | Open circuit voltage $U_{x.x}$, V | Operating current $I_{oc}$, A | | Energy of discharge $W_u$, J | |
|---|---|---|---|---|---|
| | | $C = 150$ μF | $C = 300$ μF | $C = 150$ μF | $C = 300$ μF |
| 3 | 30 | 0.5–0.6 | 1.6–2.0 | 0.04 | 0.08 |
| 5 | 47 | 0.7–0.8 | 2.0–2.2 | 0.10 | 0.20 |
| 7 | 67 | 0.9–1.0 | 2.4–2.7 | 0.20 | 0.40 |
| 9 | 87 | 1.1–1.3 | 2.6–3.5 | 0.34 | 0.68 |

**Table 2.** Series of studied specimens

| Specimen no. | Material | |
|---|---|---|
| | base | coating |
| 1 | Steel 20 | Copper (ESA)–tin (ESA) |
| 2 | Steel 20 | Copper (ESA)–tin (plating) |
| 3 | Steel 20 | Bronze (ESA)–tin (ESA) |
| 4 | Steel 20 | Bronze (ESA)–tin (plating) |
| 5 | Steel 20–tin (plating)–babbit | Indium (ESA) |
| 6 | Steel 20–tin (plating)–babbit | Tin (ESA) |

restricted by the effectiveness of the method; an increase in the discharge energy to above 0.03 J during the deposition of indium or tin leads to rapid heating, loss of the shape of the indium electrode, and a drastic increase in the roughness of the alloyed surface when using a tin electrode.

Spinning the babbit layer on a steel base warmed up to 100–120°C and preliminarily cleaned and degreased was carried out using a lathe. The temperature of babbit during spinning was 420 ± 10°C. The base of the bearing was mounted in a lathe chuck and sealed by a protective sleeve. The babbit was lined by a short continuous jet. The thickness of the babbit layer was 2–2.5 mm, while after mechanical treatment it became 1.5–0.2 mm [6].

The metallographic studies were conducted on a Neofot-2 optical microscope and a JOEL LSM-540 raster electron microscope. The layer's continuity and the thickness and structure of the sublayer, namely, the diffusion zone and thermal impact area, were evaluated. The distribution of microhardness by depth in the surface layer was studied on a PMT-3 microhardness meter at various loads. To investigate the distribution of elements by the depth of the layer, X-ray spectral microanalysis, which is based on the detection of intrinsic X-ray radiation excited by the electron mean of the chemical elements present in the excitation microvolume, was performed. In this case, an electron microscope, the ISIS 300 Oxford Instruments microanalyzer, was used.

To test the adhesive strength of the babbit layer (B83 and B88) to the substrate, tests according to GOST ISO 4386-2-99 were carried out. For this purpose, friction bearings with a size of ∅100/∅80 mm, $b = 45$ mm with antifriction layers on the internal surface of the following four compositions were made:

(1) Steel 20–tin plating–babbit spinning (conventional technology);

(2) BrOTsS 5-5-5 bronze–tin plating–babbit spinning;

(3) Steel 20–ESA by M1 copper–tin plating–babbit spinning;

(4) Steel 20–ESA by BrOTsS 5-5-5 bronze–tin plating–babbit spinning.

Electric-spark alloying by copper and bronze was performed under an argon atmosphere. In this case, the mode with the discharge energy of 0.34 J was used. As electrodes, rods with a diameter of 3 mm of M1 copper and BrOTsS 5-5-5 bronze were employed. The diagram of the setup for the adhesive strength test of the antifriction layer to the base and the size of test specimens prepared from a steady bush are given in Fig. 1.

## RESULTS

### *Coatings in the Contact Area of Babbit with the Metal Base*

The mass transfer of copper and bronze to a steel substrate during electric-spark alloying was investigated. The experiments showed that both in the air and in an argon atmosphere the amount of the material transferred from the anode to the cathode

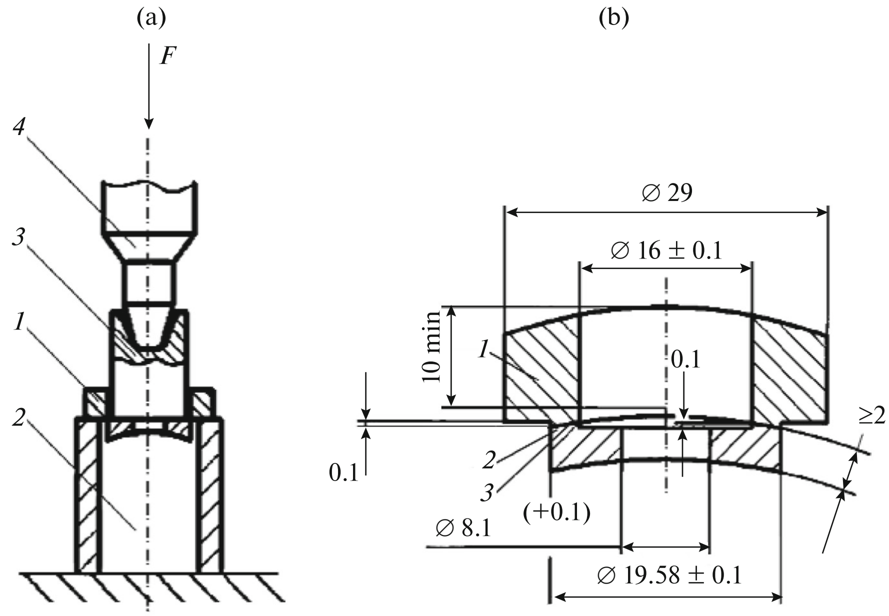


**Fig. 1.** (a) Strength test device of joint of antifriction layer with base: (*1*) test specimen; (*2*) steady bush; (*3*) coupling; (*4*) push bar; (b) test specimen: (*1*) base, (*2*) babbit, and (*3*) test transition layer.

increases with an increase in the discharge energy. The most intense mass transfer occurs at the start of alloying; then, it slows and is gradually replaced by the erosion of the layer deposited earlier. During alloying in a protective atmosphere, the mass transfer is higher when the other conditions are the same. This primarily indicates that metal oxide in the alloying area prevents the formation of a surface layer.

The results of the measurements of the roughness and thickness of the surface, as well as the coefficient ($K_m = \Delta P_{argon}/\Delta_{air}$), which considers the gain ratio of the cathode during ESA in argon and air for 1 min, are given in Table 3. It was determined that there is a rational time of alloying for each operating condition ($t_{rat}$), which is necessary to obtain a sound coating. In this case, the preparation of 100%-continuous coatings was taken as the criterion of the choice of the alloying period.

Copper and tin bronze electrodes are gradually oxidized, which affects the quality of the formed coatings. Burns arise, electrodes are mechanically destroyed, and individual particles with sizes of up to 0.2–0.5 mm stick to the alloyed surface. This is clear during long-term alloying in the air. In an argon atmosphere, there is practically no oxidation. During operation, the electrode surface, which is brought into contact with the alloyed surface, was cleaned from oxides from time to time.

It was determined that the best quality of the coating (continuity, roughness, and homogeneity) is achieved during the deposition of coatings in argon at

**Table 3.** Parameters of surface layers during ESA of steel 20 by copper and tin bronze

| Mode | | $t_{rat}$, min Argon/air | Roughness $R_z$, μm | | | | Increment $\Delta h$, mm | | | | $K_m$, times | |
|---|---|---|---|---|---|---|---|---|---|---|---|---|
| | | | copper | | bronze | | copper | | bronze | | | |
| | | | air | argon | air | argon | air | argon | air | argon | copper | bronze |
| 150 μF | 3 | 2.5/3.0 | 8 | 7 | 10 | 7 | 0.025 | 0.01 | 0.04 | 0.02 | 0.75 | 1.6 |
| | 5 | 1.5/2.0 | 10 | 8 | 12 | 8 | 0.04 | 0.02 | 0.06 | 0.03 | 1.2 | 1.5 |
| | 7 | 1.0/1.2 | 12 | 9 | 14 | 9 | 0.05 | 0.02 | 0.07 | 0.03 | 1.3 | 2.3 |
| | 9 | 0.75/1.0 | 15 | 10 | 17 | 11 | 0.07 | 0.03 | 0.08 | 0.04 | 1.5 | 1.36 |
| 300 μF | 3 | 1.5/2.0 | 9 | 7 | 11 | 8 | 0.01 | 0.01 | 0.01 | 0.01 | 1.0 | 2.0 |
| | 5 | 1.0/1.2 | 12 | 8 | 14 | 9 | 0.05 | 0.02 | 0.07 | 0.02 | 1.1 | 2.0 |
| | 7 | 0.8/1.1 | 16 | 9 | 19 | 10 | 0.09 | 0.03 | 0.11 | 0.04 | 1.3 | 1.9 |
| | 9 | 0.5/0.75 | 27 | 11 | 30 | 12 | 0.14 | 0.04 | 0.17 | 0.05 | 1.2 | 1.15 |

the discharge energy of 0.2–0.4 J, which provides 100% continuity and roughness $R_z$ = 8–10 μm. During ESA in the air, the thickness of the formed layers takes values of 30–70 μm in the case of copper and 30–80 μm in the case of tin bronze depending on the mode. The layer continuity is ~90%. In an argon atmosphere, the continuity of the layer increases significantly, and its thickness after ESA in the same modes is 20–30 μm in the case of copper and 30–40 μm in the case of tin bronze. The layer continuity in this case is almost 100% for both electrode materials and the alloying conditions used.

Investigation of the structure of electric-spark coatings showed that the surface layer of steel 20 with a copper or tin bronze coating both in the air and in an argon atmosphere consists of two zones: a white layer near the surface and a transition layer underneath it. The presence and depth of the third layer with increased microhardness represented by the thermal impact area (TIA) depend on the energy of the spark discharge.

The durometric analysis shows that during alloying by copper and tin bronze in various media, the microhardness on the layer surface is 850–900 and 1050–1150 MPa, respectively. As penetration into TIA increases, it gradually grows to 2500–3000 MPa and, then, decreases to the microhardness of steel (1750–1800 MPa). The TIA thickness with the microhardness value higher than that of the main metal amounts to 50 μm during alloying in the 9th regime in the air, while under an argon atmosphere, it is 40 μm. A decrease in the TIA thickness upon alloying under an argon atmosphere compared to alloying in the air is caused by the cooling of the ESA zone by the supplied gas jet. In Figs. 2a and 2c, the microstructure and microhardness distribution at the boundary between steel 20 and tin, which were deposited using a conventional plating technique, are given. The transition layer between tin and the substrate (steel 20) is absent. The microhardness value drastically changes from 310–340 (tin) to 1750–1800 MPa (steel 20). In this case, tin is retained on the steel substrate only due to adhesion.

During the ESA of steel 20 by copper or tin bronze, substitutional solid solutions are formed between tin and copper or copper and the components of tin bronze in the diffusion area, which provide stronger adhesion. Microhardness in the transition layer initially gradually increases from 210–230 (tin) to 2700–2800 MPa (TIA) and, then, gradually decreases to the microhardness of the base (Figs. 2b, 2c).

In Fig. 3a, the most intrinsic section of the surface layer of steel 20 after ESA by copper and tin in the plane that is orthogonal to the coating is given. The formed surface layer consists of two zones. On the surface, there is a tin layer with a thickness of 10–15 μm. The layer below consists mainly of copper with a thickness of 15–20 μm. There are closed pores with sizes from fractions to 3 μm both in the first and second layers, while the larger pores are in the copper layer. Investigation of the composition of the coating by depth proves that the boundary sections between tin, copper, and steel 20 consist of elements of the neighboring layers, which indicates their diffusional rearrangement in the coating. As the penetration increases, the concentration of copper grows in the lower tin layers. On the boundary between copper and steel, the concentration of copper decreases, while that of iron increases.

When there is ESA of steel by copper and further tin plating (Fig. 3b) no significant differences in the structure of the formed surface layer are observed. Studing the distribution of the elements in the coating shows the absence of a transition layer between copper and tin. In the transition area from the copper coating to the iron base, the concentration of copper decreases. At the same section, the concentration of iron increases. This confirms the intense mixing and mutual diffusion of the substrate and coating elements.

When there is a successive deposition of tin bronze and tin on steel 20 by the ESA method, the surface layer consists of two layers. The upper layer with a thickness of 15–20 μm from tin is less porous than the lower layer with a thickness of 20–30 μm from tin bronze. Transient areas between tin, tin bronze, and steel 20 consist of elements of the boundary layers. When the ESA method of tin deposition is replaced by plating, a more drastic transition from copper to tin is detected.

The results of the strength test of the joint of the antifriction layer and the metallic base are given in Table 4. In all cases, the surface area of the connection is 100 mm$^2$.

The studies showed that the application of the transient layer from copper deposited by the ESA method in a protective atmosphere (argon) increases the adhesive strength of the steel substrate with the antifriction babbit layer by 35% compared to the conventional technology (steel 20–babbit). When using the transition bronze layer, the strength grows insignificantly, while with the substitution of the bronze substrate for the steel substrate, the adhesion strength decreases.

### *Coatings on Babbit Layer Surface to Improve Running-in*

With the aim of studying the possibility to improve the running-in of friction bearings to specimens of steel 20 with the babbit layer, indium and tin coatings were deposited by ESA. As a result of indium alloying, a layer with a thickness of up to 130 μm and microhardness $H_\mu$ = 200–210 MPa is formed on the babbit surface. In this case, the microhardness of the lower babbit layers corresponds to 240–310 MPa, while that of the square-shaped solid inclusions (SnSb) is 460–

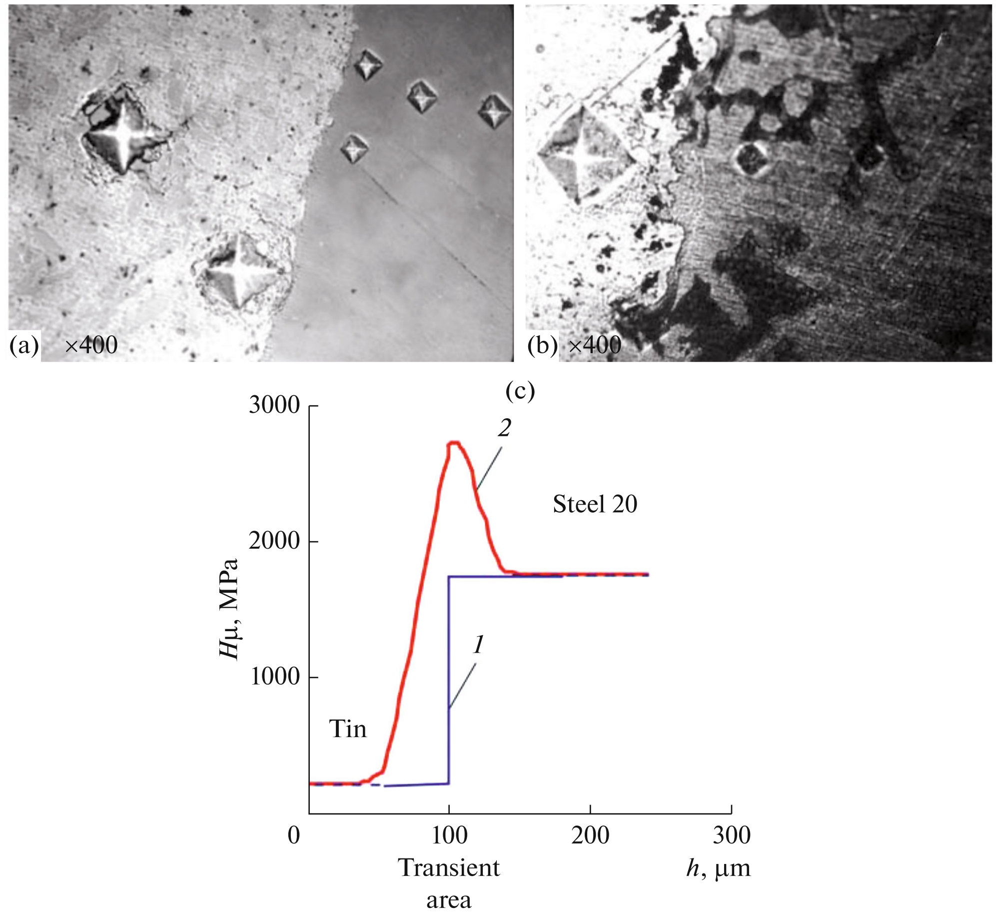


**Fig. 2.** Microstructure of (a) steel 20 and (b) with sublayer of copper (ESA) after tin plating; (c) microhardness distribution of (*1*) steel–tin and (*2*) steel–copper (ESA).

645 MPa. When the babbit surface is alloyed by tin, the depth of the running-in coating is 90–100 μm, while the microhardness is 180–190 MPa. The microhardness of the lower layers is 240–310 MPa.

In Fig. 4, the microstructure and microhardness distribution of the B83 babbit surface layer with the running-in indium coating deposited by the ESA method are given. The B83 babbit has the following

**Table 4.** Adhesion strength of antifriction layer and metal base

| Material of substrate and antrifriction layer | Adhesive strength, N/ mm$^2$ | Character of destruction |
|---|---|---|
| 1 | 2 | 3 |
| Bronze OTsS 5-5-5–tin (plating)–B83 | 18 | Break along boundary of babbit with main metal |
| Bronze OTsS 5-5-5–tin (plating)–B83 | 20 | Break along boundary of babbit with main metal |
| Steel 20–tin (plating)–B83 | 22 | Break along babbit |
| Steel 20–tin (plating)–B88 | 22 | Break along babbit |
| Steel 20+ bronze (ESA)–tin (plating)–B83 | 22 | Break along babbit |
| Steel 20+ bronze (ESA)–tin (plating)–B88 | 24 | Break along babbit |
| Steel 20+copper (ESA)–tin (plating)–B83 | 30 | Break along babbit |
| Steel 20+copper (ESA)–tin (plating)–B88 | 36 | Break along babbit |

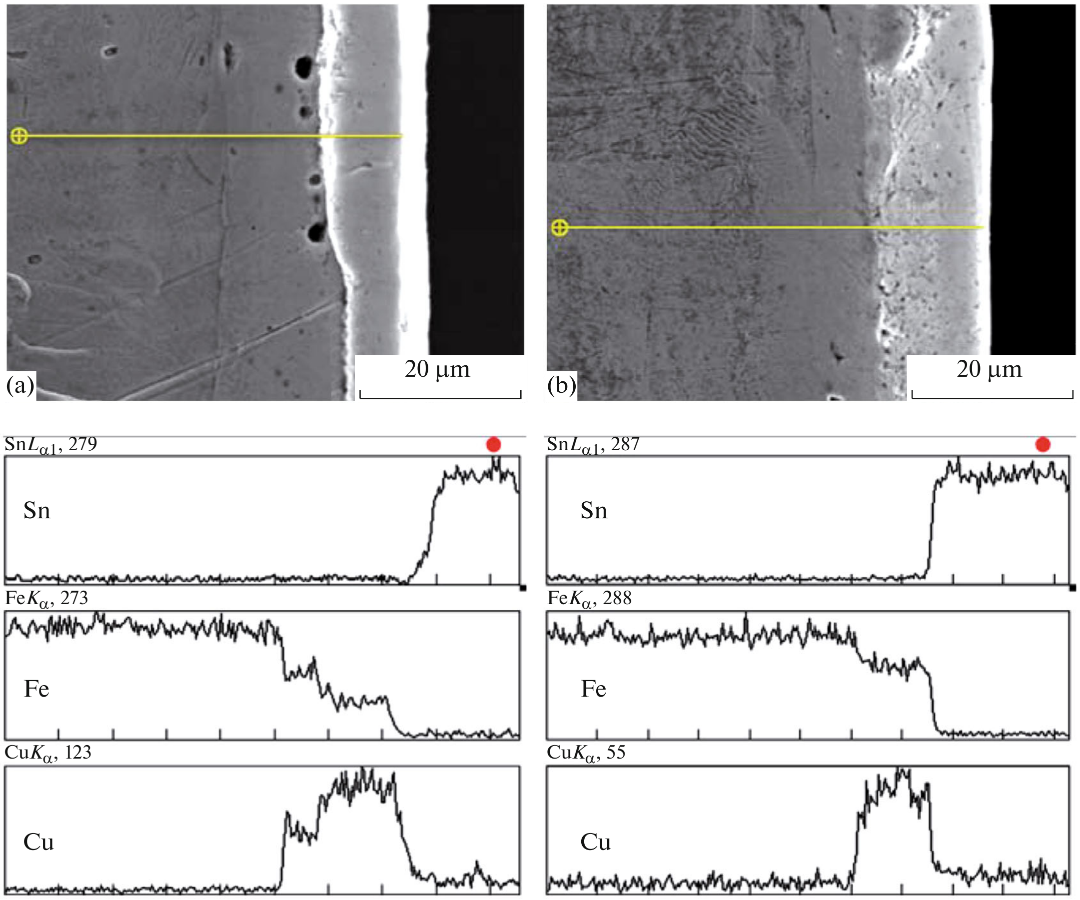


**Fig. 3.** Cross section of coatings on steel 20: (a) ESA successively with copper and tin and (b) ESA by copper followed by tin plating and distribution of Sn, Fe, and Cu by depth of coatings. ×2000.

microstructure. The dark field represents a plastic mixture of α-solid solution of antimony and copper in tin; the light square-shaped crystals correspond to an SnSb compound (β-phase); and the star-shaped or needle-like crystals correspond to a $Cu_3Sn$ compound.

In Fig. 5, the distribution of elements in the surface layer of B83 babbit after ESA by indium and tin is given. It should be noted that there are no solid inclusions of the SnSb compound (β-phase) in the structure of the running-in coatings. The produced surface layers consist of elements of the base and alloying elements. The electroerosion treatment of the B83 babbit surface by indium or tin provides the formation of the surface layer with a thickness of up to 130 and 100 μm with the microhardness softer than that of the base, which finally improves the running-in conditions of the half-bearings.

*Application of the Study Results in Industry*

The studies allowed the development of the technology to improve the quality of friction bearings of high-speed turbocompressor units by the most cost-effective methods. The new engineering solutions pro-

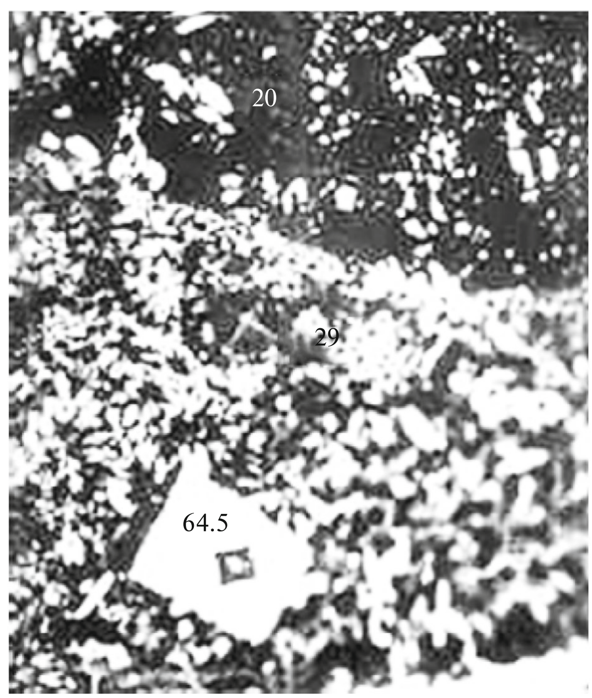


**Fig. 4.** Structure and microhardness distribution of surface layer of indium-doped B83 babbit.

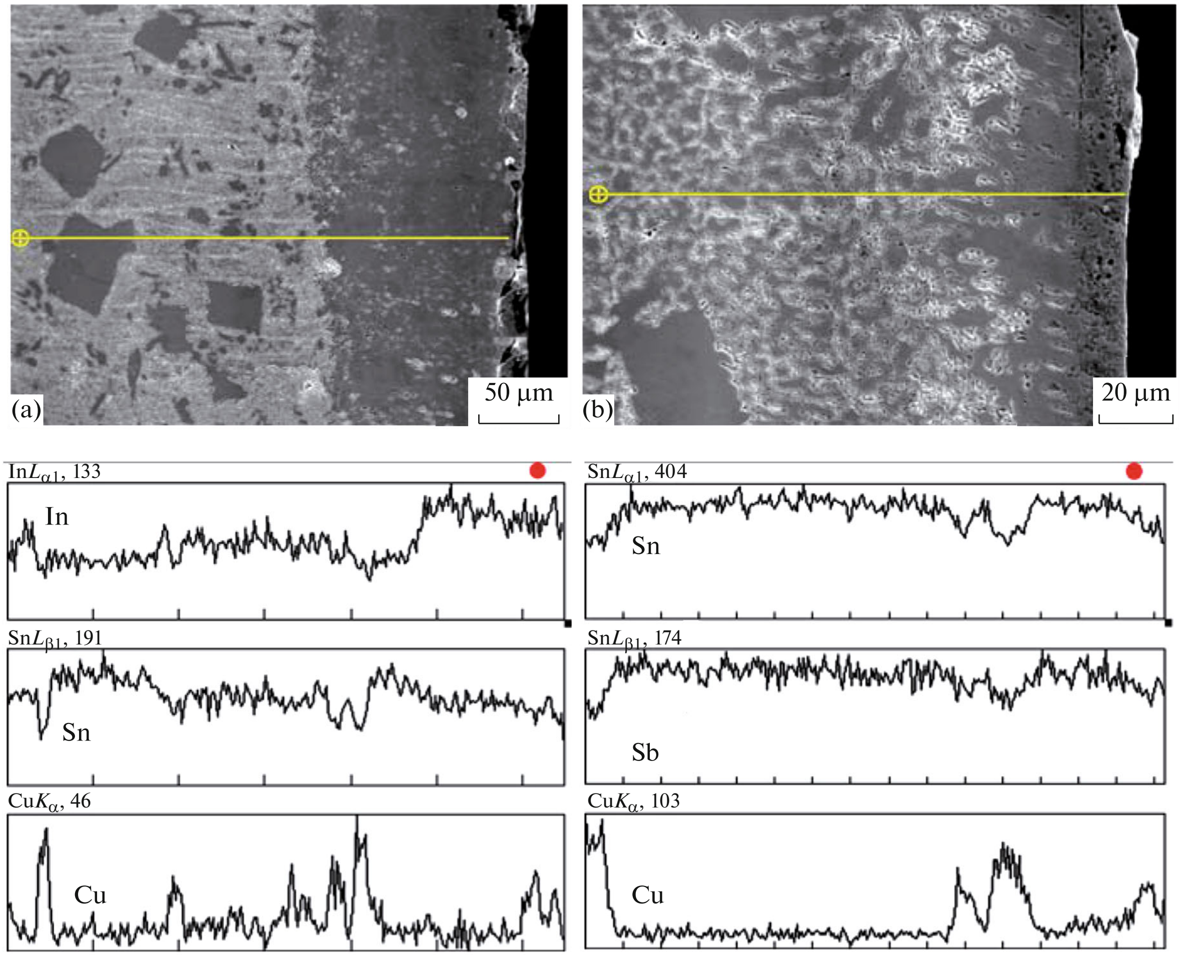


**Fig. 5.** Distribution of elements by depth of surface layer of B83 babbit after ESA by (a) indium, ×350, and (b) tin, ×750.

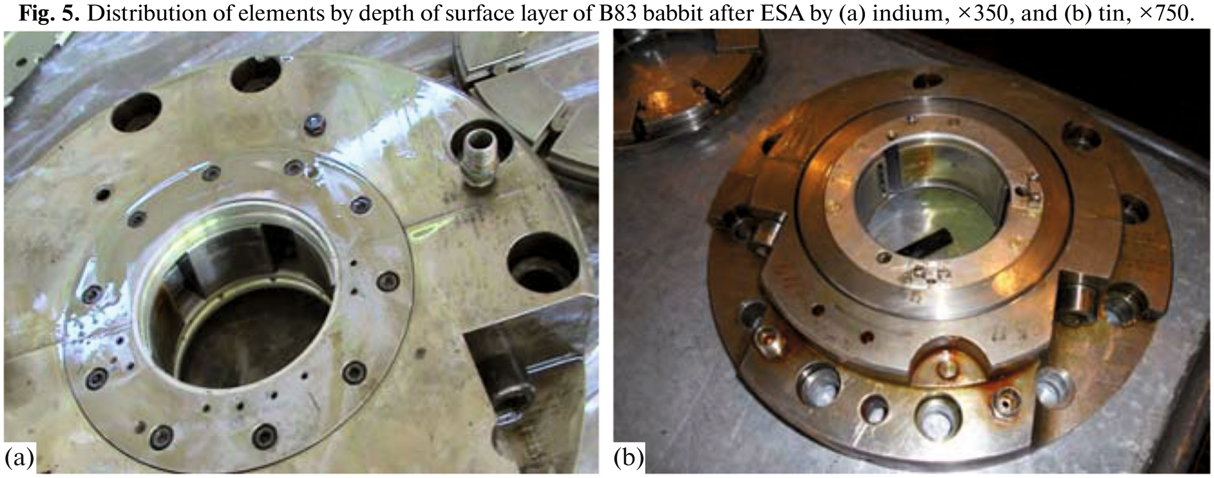


**Fig. 6.** Friction bearings of low-pressure compressor: (a) standard and (b) damping made at TRIZ enterprise.

vided the possibility to decrease the temperature in the friction area, increase the thickness of the oil layer, and thus create a bearing possessing a high load carrying ability, reliability, and cost-effective lubricant consumption, which positively affects the dynamics of the rotor and machine on the whole [7, 8].

Using the results of the studies and practical experience, damping shaft bearings are produced at the Tovarishchestvo resheniya inzhenernykh zadach (TRIZ) enterprise (Sumy, Ukraine) that possess a higher load carrying and damping ability in the entire range of operating conditions (Fig. 6). Electric-spark

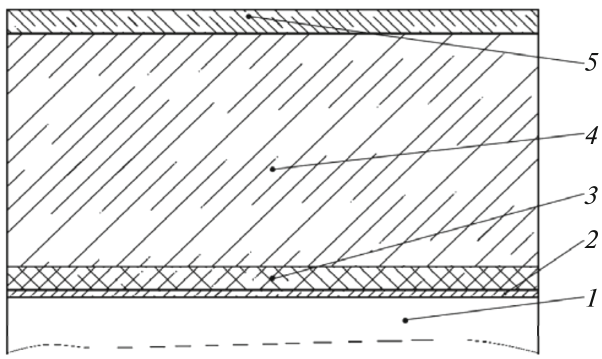


**Fig. 7.** Diagram of antifriction layer of friction half-bearings: (*1*) shoe (steel 20), 8–25 mm; (*2*) copper, 20–30 μm; (*3*) plating (tin), 80–100 μm; (*4*) babbit (B83 or B88), 1.0–1.5 mm; and (*5*) running-in coating (tin), 90–100 μm.

technologies are used for various dimensions of friction bearings, working parameters, and operating conditions on the centrifugal compressor and pumping units, turbines, and high-power electric engines.

Application of these technologies for friction bearings, floating seals, and dynamic dampers ensured a three-year warranty of the compressors of synthesis gas, which are included in the process lines of ammonia production, along with the simultaneous increase in ammonia production from 1300 to 1700 t/day. In the past, maintenance checks were considered each year with a pause of up to 30 days. Friction bearings, which possess an advanced damping ability, do well in the start-up mode; in this case, the degree of vibration decreases by a factor of up to ten. The load carrying ability of shaft bearings with electric-spark coatings are 1.5 times higher than the standard ones (Table 5).

In Fig. 7, the diagram of the antifriction layer, which is formed on the friction half-bearing, is given. During the deposition of copper and the running-in of a tin coating, the Elitron-22A and UILV-8A instruments produced in Moldova and Ukraine, respectively, are used. Tin plating and the spinning of babbit are performed by a conventional method.

The bearings with electric-spark coatings are used in the vapor turbines of synthesis gas in some enterprises in Ukraine and Russia, including Odessa's portside plant, Azot (Kemerovo), and Mineral'nye udobreniya (Perm).

## CONCLUSIONS

(1) During the investigation of the mass transfer of copper and bronze onto a steel substrate during electric-spark alloying, the optimal process conditions are determined. The thickness of the produced layers ranges from 30 to 80 μm depending on the conditions and atmosphere (air, argon) and the layer continuity is close to 100%.

(2) Investigation of the structure of the surface layer of steel with a copper or tin bronze coating shows that it consists of two zones: a white layer on the surface and a transition layer underneath it. The presence and depth of the area of the thermal impact depend on the spark discharge energy and correspond to 50 μm. The microhardness on the layer surface is 850–1150 MPa. As the penetration increases, it gradually grows to 2500–3000 MPa and then, transfers to the microhardness of the main metal (1750–1800 MPa).

(3) It is demonstrated that the application of the transition layers of copper, which is deposited by ESA under a protective argon atmosphere, improves the heat withdrawal from the contact area and increases the adhesive strength of the steel substrate to the antifriction babbit layer compared to the conventional technology by 35%. With the substitution of a bronze substrate for steel, the adhesive strength decreases.

(4) It is determined that ESA of the B83 babbit surface by indium or tin provides the formation of running-in coatings without solid inclusions with a thickness of up to 130 and 100 μm, respectively.

(5) The new technological solutions provide a decrease in temperature in the friction area, increase the thickness of the oil layer, and thus create a bearing possessing a high load carrying ability, reliability, and cost-effective consumption of the lubricant. At the Tovarishchestvo resheniya inzhenernykh zadach (TRIZ) enterprise (Sumy, Ukraine), shaft bearings are produced that possess a higher load carrying and damping ability than the standard bearings and are successfully used in compressors at several enterprises in Ukraine and Russia.

**Table 5.** Comparative characteristics of 130JT turbine bearings

| Modification of bearings | Load carrying ability *F*, kgf | Specific pressure *P*, kgf/cm$^2$ | Specific consumption of lubricant θ, L/min t | Vibration of rotor δ, μm |
|---|---|---|---|---|
| Standard bearings PO120 | 2300 | 28 | 15 | 35 |
| Bearings with electric-spark coatings PD120 | 3600 | 42 | 11 | 7 |

## REFERENCES


1. Potekhin, B.A., Il'yushin, V.V., and Khristolyubov, A.S., *Met. Sci. Heat Treat.*, 2009, 51, no. 8, p. 378.
2. Barykin, N.P., Fazlyakhmetov, R.F., and Valeeva, A.Kh., *Met. Sci. Heat Treat.*, 2006, vol. 48, no. 1, pp. 88–91.
3. Kukushkin, E.V., Menovshchikov, V.A., and Eresko, T.T., *Mater. X Vseross. nauchno-prakt. konferentsii tvorcheskoi molodezhi "Aktual'nye problemy aviatsii i kosmonavtiki," Tezisy dokladov* (Proc. 10th All-Russ. Sci.-Pract. Conf. of Creative Youth "Modern Aviation and Space Science," Abstracts of Papers), Krasnoyarsk, 2014, vol. 1, pp. 148–150.
4. Tarel'nik, V.B. and Dzyuba, O.V., *Visn. Khark. Nats. Tekh. Univ. Sil'sk. Gospod. im. Petra Vasilenka*, 2013, no. 134 pp. 244–251.
5. Chichinadze, A.V., Berlinger, E.M., Brown, E.D., et al., *Trenie, iznos i smazka* (Friction, Wear, and Lubrication), Moscow: Mashinostroenie, 2003.
6. Galiakhmetov, I.G., *Konstruktsionnye materialy tsentrobezhnykh i vintovykh kompressorov. Vybor i tekhnologiya ikh primeneniya* (Construction Materials of Centrifugal and Screw Compressors: Choice and Application Technology), Kazan: Fon, 2009.
7. Martsinkovs'kii, V.S. and Tarel'nik, V.B., UA Patent 92814, *Byull. Izobret.*, 2010, no. 23.
8. Martsinkovs'kii, V.S. and Tarel'nik, V.B., RU Patent 2404378, *Byull. Izobret.*, 2010, no. 32.


*Translated by A. Muravev*